Genipin-crosslinked silk fibroin/hydroxybutyl chitosan nanofibrous scaffolds for tissue-engineering application

Kuihua Zhang,[1,2,3,4] Yongfang Qian,[1,3] Hongsheng Wang,[3] Linpeng Fan,[3] Chen Huang,[1,2] Anlin Yin,[3] Xiumei Mo[1,2,3]

[1]Key Laboratory of Textile Science and Technology Ministry of Education, Donghua University, Shanghai 201620, People's Republic of China
[2]State Key Laboratory for Modification of Chemical Fibers and Polymer Materials, College of Materials Science and Engineering, Donghua University, Shanghai 201620, People's Republic of China
[3]Biomaterials and Tissue Engineering Laboratory, College of Chemistry and Chemical Engineering and Biological Engineering, Donghua University, Shanghai 201620, People's Republic of China
[4]College of Biological Engineering and Chemical Engineering, Jiaxing College, Zhejiang 314001, People's Republic of China

Received 23 January 2010; revised 18 April 2010; accepted 21 May 2010
Published online 7 September 2010 in Wiley Online Library (wileyonlinelibrary.com). DOI: 10.1002/jbm.a.32895

Abstract: To improve water-resistant ability and mechanical properties of silk fibroin (SF)/hydroxybutyl chitosan (HBC) nanofibrous scaffolds for tissue-engineering applications, genipin, glutaraldehyde (GTA), and ethanol were used to crosslink electrospun nanofibers, respectively. The mechanical properties of nanofibrous scaffolds were obviously improved after 24 h of crosslinking with genipin and were superior to those crosslinked with GTA and ethanol for 24 h. SEM indicated that crosslinked nanofibers with genipin and GTA vapor had good water-resistant ability. Characterization of the microstructure (porosity and pore structure) demonstrated crosslinked nanofibrous scaffolds with genipin and GTA vapor had lager porosities and mean diameters than those with ethanol. Characterization of FTIR-ATR and ^{13}C NMR clarified both genipin and GTA acted as crosslinking agents for SF and HBC. Furthermore, genipin could induce SF conformation from random coil or α-helix to β-sheet. Although GTA could also successfully crosslink SF/HBC nanofibrous scaffolds, in long run, genipin maybe a better method due to lower cytotoxicity than GTA. Cell viability studies and wound-healing test in rats clarified that the genipin-crosslinked SF/HBC nanofibrous scaffolds had a good biocompatibility both *in vitro* and *in vivo*. These results suggested that genipin-crosslinked SF/HBC nanofibrous scaffolds might be potential candidates for wound dressing and tissue-engineering scaffolds. © 2010 Wiley Periodicals, Inc. J Biomed Mater Res Part A: 95A: 870–881, 2010.

Key Words: electrospinning, crosslink, genipin, tissue engineering

INTRODUCTION

The native ECM is composed of a cross-linked porous network of multifibrils collagens with diameters ranging from 500 nm to 15 μm and embedded in glycosaminoglycans.[1–3] Biomimic nonwoven scaffolds generated by electrospinning have been composed of a large network of interconnected fibers and pores, resembling the topographic features of the ECM.[4] The electrospun nanofibers of silk fibroin (SF) and chitosan blends are expected to better biomimic the ECM of native tissues. Hydroxybutyl chitosan (HBC) is fabricated by conjugation of hydroxybutyl (HB) groups to the hydroxyl and amino reactive sites of chitosan. This modification could increase the solubility of chitosan in water or organic solution and electrospinability of chitosan,[5] while still remain excellent properties of chitosan.[6,7] However, electrospun SF/HBC nanofibrous scaffolds are easily dissolved or swelled in water. Therefore, successful crosslinking is needed to increase the stability of scaffolds both *in vivo* and *in vitro*. According to literature, pure SF electrospun nanofibrous scaffolds were treated with methanol, ethanol, or water vapor to improve stability both *in vivo* and *in vitro*[8,9] while pure chitosan or its blends electrospun nanofibrous scaffolds were generally crosslinked with glutaraldehyde (GTA).[10,11]

Genipin is a naturally occurring crosslinking agent that is derived from the fruits *Genipa Americana* and *Gardenia jasminoides Ellis* and has recently been used for its ability to crosslink CS and proteins containing residues with primary amine groups.[12,13] Meanwhile, Tsai et al.[14] reported that genipin was an effective cross-linker that improved materials mechanical properties and possessed particularly lower cytotoxicity than GTA. Some reports have demonstrated that chitosan/SF sponges and patches crosslinked with genipin

Correspondence to: X. Mo; e-mail: med@dhu.edu.cn
Contract grant sponsor: National High Technology Research and Developed Program (863 Program); contract grant number: 2008AA03Z305
Contract grant sponsor: Science and Technology Commission of Shanghai Municipality Program; contract grant numbers: 08520704600, 0852nm03400
Contract grant sponsor: "111 Project" Biomedical Textile Materials Science and Technology; contract grant number: B07024
Contract grant sponsor: Shanghai-Unilever Research and Development Fund; contract grant number: 08520750100

could improve their stability and have good biocompatibility.[15,16] However, crosslinking of SF/chitosan nanofibrous scaffolds has not been reported.

In this study, to improve water stability of fibers, SF/HBC nanofibers were fabricated and crosslinked with genipin. GTA and ethanol were used for comparison. The morphology, structure, and mechanical properties of crosslinked nanofibrous scaffolds were investigated. To assess the cytocompatibility and cells behavior on electrospun scaffolds, the viability of pig iliac endothelial cells (PIECs) on crosslinked SF/HBC nanofibrous scaffolds were studied. Meanwhile, crosslinked SF/HBC nanofibrous scaffolds were implanted into the standard deviation (SD) rats for wound dressing to evaluate the biocompatibility *in vivo*.

MATERIALS AND METHODS

Materials

Cocoons of Bombyx mori silkworm were kindly supplied by Jiaxing Silk Co. (China). HBC was kindly provided by Shanghai Qisheng biological agents Co. (China) Two kinds of solvents, 1,1,1,3,3,3-hexafluoroisopropanol (HFIP) from Fluorochem (United Kingdom) and trifluoroacetic acid (TFA) from Sinopharm Chemical Reagent Co. (China). Genipin (purity: HPLC $>$ 98%; soluble in alcohol) from Shanghai Hulun Pharmaceutical Co. (China).

Preparation of regenerated SF

Raw silk was degummed three times with 0.5% (w/w) Na_2CO_3 solution at 100°C for 30 min each and then washed with distilled water. Degummed silk was dissolved in a ternary solvent system of $CaCl_2/H_2O/EtOH$ solution (1/8/2 in mol ratio) for 1 h at 70°C. After dialysis with cellulose tubular membrane (250-7u; Sigma) in distilled water for 3 days at room temperature, the SF solution was filtered and lyophilized to obtain the regenerated SF sponges.

Electrospinning of SF/HBC nanofibers

The SF was dissolved in HFIP for 12 w/v % concentration and HBC was dissolved in HFIP/TFA mixture (v/v 90:10) for 6 w/v % concentration, respectively. When they were prepared already, the two solutions were blended at different weight ratios with sufficient stirring at room temperature before electrospinning. The solutions were placed into a 2.5-mL plastic syringe with a blunt-ended needle with an inner diameter of 0.21 mm. The needle was located at a distance of 150 mm from the grounded collector. A syringe pump (789100C, cole-pamer, America) was used to feed solutions to the needle tip at a feed rate of 0.5–1.0 mL/h. A high-electrospinning voltage was applied between the needle and ground collector using a high-voltage power supply (BGG6-358, BMEICO, China). The applied voltage was 20 kV. The electric field generated by the surface charge caused the solution drop at the tip of the needle to distort into a Taylor cone.

Crosslinking and water-resistant test

Genipin was dissolved in ethanol with the concentration of 50 mg/mL, and then 20-mL genipin solution, 20-mL pure ethanol, and 20 mL 25w/v % GTA water solution were put into a desiccator, respectively. Fixed SF/HBC nanofibrous scaffolds were placed in a desiccator saturated with different vapor at room temperature (30°C or so) for different time and then dried in a vacuum at room temperature for 1 week, respectively. SF/HBC nanofibrous scaffolds after crosslinking were soaked in deionized water for 4 days, and nanofibrous scaffolds were dried in a vacuum oven for 1 week and then observed by SEM.

Characterization

The morphology of SF/HBC nanofibrous scaffolds was observed with a scanning electronic microscope (SEM) (JSM-5600, Japan) at an accelerated voltage of 10 kV.

The Fourier transform infrared attenuated total reflectance spectroscopy (FTIR-ATR) spectra were obtained at room temperature in on AVATAR 380 FTIR instrument (Thermo Electron, Waltham, MA) in the range 4000–600 cm^{-1} at a resolution of 4 cm^{-1}.

The ^{13}C CP-MAS NMR spectra of SF/HBC nanofibrous scaffolds were obtained on NMR spectrometer (Bruker AV400, Switzerland) with a ^{13}C resonance frequency of 100 MHz, contact time of 1.0 ms, and pulse delay time of 4.0 s.

Pore size and porosity measurements

An CFP-1100-AI capillary flow porometer (PMI Porous Materials Int.) was used in this study to measure the pore size. Calwick with a defined surface tension of 21 dynes/cm (PMI Porous Materials Int.) was used as the wetting agent for porometry measurements. Electrospun nanofibrous scaffolds were cut into 3 cm $\times$ 3 cm squares for porometry measurement.

The porosities of eletrospinning nanofibrous scaffolds before and after crosslinking were generally calculated using the listed formula.[17] The nanofibrous scaffold was cut into 3 cm $\times$ 3 cm squares, and the thickness was measured with a micrometer (Shanghai, China).

$$\text{Apparent density of nanofibrous scaffold}(\text{g/cm}^3) = \frac{\text{Mass of nanofibrous scaffold}(\text{g})}{\text{Scaffold thickness}(\text{cm}) \times \text{area}(\text{cm}^2)}$$

$$\text{Porosity of nanofibrous scaffold}\ (\%) = \left(1 - \frac{\text{Nanofibrous scaffold apparent density}(\text{g/cm}^3)}{\text{Bulk density of raw SF/HBC}(\text{g/cm}^3)}\right)$$

In this study, both SF and HBC are porous materials, and so it is extremely difficult to precisely measure their bulk densities. As a result, porosity analysis may be a certain extent errors.

Mechanical measurements

Mechanical properties were obtained by applying tensile test loads to specimens prepared from the electrospun scaffolds. In this study, specimens were prepared according to the method described by Huang et al.[18] First, a white paper was cut into template with width $\times$ gauge length, and double-side tapes were glued onto the top and bottom areas of one side. The template was then glued onto top side of the fiber scaffold and

cut into rectangular pieces along the vertical lines. After the aluminum foil was carefully peeled off, single side tapes were applied onto the gripping areas as end-tabs. The resulting specimens had a planar dimension of width × gauge length = 10 mm × 30 mm. Mechanical properties were tested by a materials testing machine (H5K-S, Hounsfield, England) at the temperature of 20°C and a relative humidity of 65% and a elongation speed of 10 mm/min. The specimen thicknesses were measured using a micrometer having a precision of 0.01 mm. The machine-recorded data were used to process the tensile stress–strain curves of the specimens.

Viability study of PIEC on nanofibrous scaffolds

Pig iliac endothelial cells (PIECs) were cultured in DMEM medium with 10% fetal bovine serum and 1% antibiotic–antimycotic in an atmosphere of 5% CO_2 and 37°C, and the medium was replenished every 3 days. Electrospun scaffolds were prepared on circular glass coverslips (14 mm in diameter) and fixed by different vapor and then placed the coverslips into 24-well plates with stainless ring. Before seeding cells, scaffolds were sterilized by immersion in 75% ethanol for 2 h, washed three times with phosphate-buffered saline solution (PBS), and then washed once with the culture medium.

Cells viability on electrospun scaffolds, coverslips, and tissue culture plates (TCP) were determined by MTT method. Briefly, the cell and SF matrices were incubated with 5 mg/mL 3-[4, 5-dimehyl-2-thiazolyl]-2,5-diphenyl-2H-tetrazolium bromide (MTT) for 4 h. Thereafter, the culture media were extracted and added 400 μL dimethylsulfoxide for about 20 min. When the crystal was sufficiently resolved, aliquots were pipetted into the wells of a 96-well plate and tested by an Enzyme-labeled Instrument (MK3, Thermo, USA), and the absorbance at 490 nm for each well was measured.

For the proliferation study, endothelial cells were seeded onto nanofibrous scaffolds, glass coverslips, and TCP ($n = 4$) at a density of 1.0×10^4 cells/well for 1, 3, 5, and 7 days. After cell seeding, unattached cells were washed out with PBS solution, and attached cells were quantified by MTT method.

After 3 days of culturing, the electrospun fibrous scaffolds with cells (density is 1.0×10^4 cells/well) were examined by SEM. The scaffolds were rinsed twice with PBS and fixed in 4% GTA water solution at 4°C for 2 h. Fixed samples were rinsed twice with PBS and then dehydrated in graded concentrations of ethanol (30, 50, 70, 80, 90, 95, and 100%). Finally, they were dried in vacuum overnight. The dry cellular constructs were coated with gold sputter and observed under the SEM at a voltage of 10 kV.

Wound-healing test

Wound-healing test was carried out with animal models using SD rats. A full thickness wound with a surface area of 2 cm × 2 cm was cut from the back of the SD rat, parallel with the vertebral column. The wound was covered with an equal size of electrospun SF/HBC scaffolds crosslinked with genipin vapor. The same wound was treated with cotton gauze as a control. The area of the wound was evaluated at 1 and 3 weeks for histological examination, tissue specimens from animal wounds were obtained and fixed in 10% neutral-buffered formalin solution, embedded in paraffin wax, sectioned at 3 μm, and stained with hematoxylin-eosin (H-E) in the conventional manner.

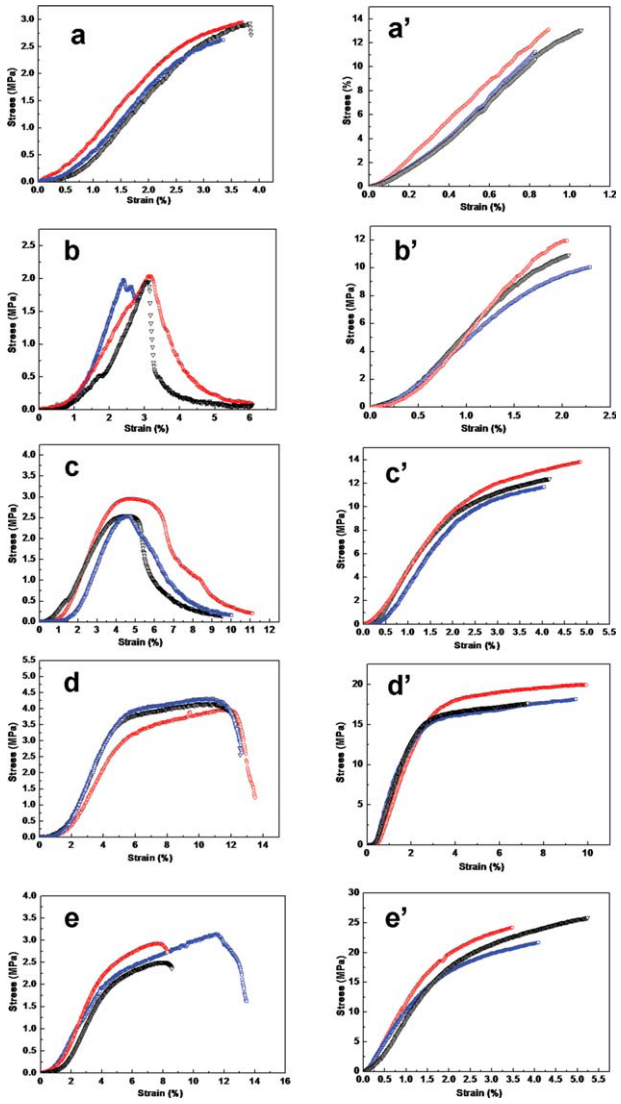

FIGURE 1. The stress-strain curves of SF/HBC nanofibrous scaffolds with different weight ratios before and after crosslinking with genipin vapor. (a, a′) 100:0; (b, b′) 80:20; (c, c′) 50:50; (d, d′) 20:80; (e, e′) 0:100. [Color figure can be viewed in the online issue, which is available at wileyonlinelibrary.com.]

Statistics analysis

Statistics analysis was performed using origin 7.5 (Origin Lab, USA). Values (at least triplicate) were averaged and expressed as mean ± SD. Statistical differences were determined by the analysis of one-way ANOVA, and differences were considered statistically significant at $p < 0.05$.

RESULTS AND DISCUSSION

Mechanical properties of crosslinked SF/HBC nanofibers scaffolds

The typical tensile stress–strain curves of SF/HBC nanofibrous scaffolds with different weight ratios before and after

TABLE I. Mechanical Properties of SF/HBC Nanofibrous Scaffolds With Various Blend Ratios

SF/HBC Weight Ratio		Average Specimen Thickness (mm)	Average Elongation at Break (%)	Average Tensile Strength (MPa)
100:0	Noncrosslinked	0.050 ± 0.005	3.85 ± 0.30	2.72 ± 0.60
	Crosslinked	0.057 ± 0.008	0.93 ± 0.11	12.48 ± 1.05
80:20	Noncrosslinked	0.163 ± 0.021	2.89 ± 0.41	1.99 ± 0.04
	Crosslinked	0.059 ± 0.016	2.13 ± 0.13	11.00 ± 0.96
50:50	Noncrosslinked	0.169 ± 0.023	4.70 ± 0.10	2.68 ± 0.24
	Crosslinked	0.061 ± 0.011	4.33 ± 0.45	12.66 ± 1.12
20:80	Noncrosslinked	0.068 ± 0.014	11.04 ± 0.88	4.35 ± 0.45
	Crosslinked	0.047 ± 0.007	8.88 ± 1.42	18.65 ± 1.22
0:100	Noncrosslinked	0.060 ± 0.004	9.34 ± 3.04	2.66 ± 0.20
	Crosslinked	0.049 ± 0.005	4.26 ± 0.89	23.86 ± 1.99

Data are representatives of six independent experiments and all date are used as mean ± SD.

crosslinking with genipin for 24 h were shown in Figure 1. The average elongation at break and average tensile strength of each specimen were summarized in Table I. The pure SF nanofibrous scaffolds showed typical brittle fracture and average elongation at break was only 3.85 ± 0.30%, and average tensile strength was 2.72 MPa ± 0.60. As the blend ratios of SF /HBC were 80:20 and 50:50, the stress of nanofibrous scaffolds gradually increased to 1.99 and 2.68 MPa and then began to decrease, respectively. In experiment, we found that the nanofibrous scaffolds were so loose, so that some parts of them were torn when stretched. This may be caused by the slippage among nanofibers rather than the break of fibers. Both the tensile strength and elongation at break were improved obviously when the ratio of SF to HBC was 20:80. After crosslinking with genipin for 24 h, SF/HBC nanofibrous scaffolds with different weight ratios possessed much higher tensile strength and lower elongation at break in comparison with noncrosslinked scaffolds. This was mainly caused by the intermolecular and intramolecular covalent bonds and the physical entanglements formed among nanofibers, whereby the decrease of sliding in chains and among fibers led to

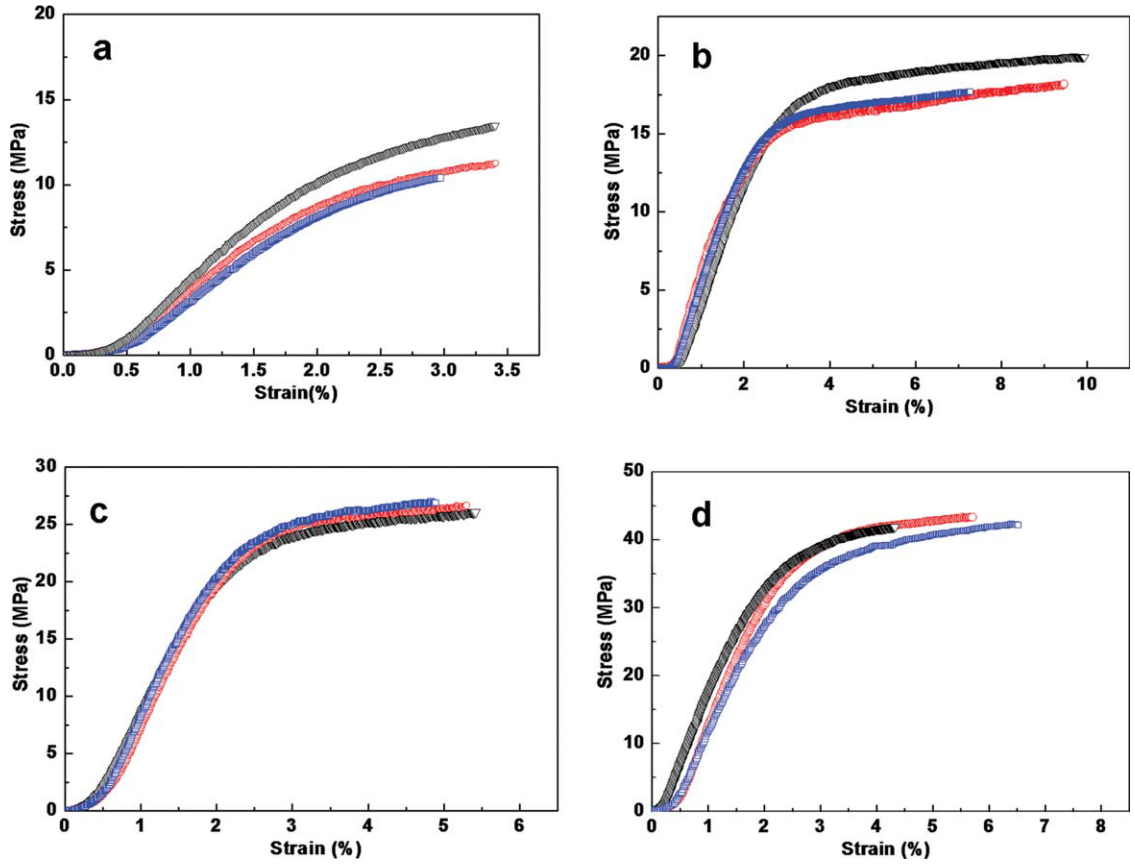

FIGURE 2. The stress-strain curves of SF/HBC nanofibrous scaffolds after crosslinking with genipin vapor for different time. (a) 12 h; (b) 24 h; (c) 48 h; (d) 72 h. [Color figure can be viewed in the online issue, which is available at wileyonlinelibrary.com.]

TABLE II. Mechanical Properties of SF/HBC Nanofibrous Scaffolds After Crosslinking Different Time and Crosslinkers

Crosslinking Agents and Time	Average Specimen Thickness (mm)	Average Elongation at Break (%)	Average Tensile Strength (MPa)
Genipin 12 h	0.049 ± 0.007	3.09 ± 0.37	11.44 ± 1.37
Genipin 24 h	0.047 ± 0.007	8.88 ± 1.42	18.65 ± 1.22
Genipin 48 h	0.036 ± 0.002	5.19 ± 0.27	26.72 ± 0.43
Genipin 72 h	0.026 ± 0.005	5.11 ± 0.84	39.53 ± 6.29
TGA 24 h	0.051 ± 0.010	3.20 ± 0.37	16.71 ± 0.40
Ethanol 24 h	0.042 ± 0.004	5.45 ± 0.60	21.07 ± 0.55

Data are representatives of six independent experiments and all date are used as mean ± SD.

significantly improved overall tensile strength. Among nanofibrous scaffolds with different weight ratios, nanofibrous scaffolds with the ratio of 20:80 had better mechanical properties after crosslinking. That is why we selected nanofibrous scaffolds with the ratio of 20:80 as following tensile properties study. The stress–strain curves of SF/HBC nanofibrous scaffolds after crosslinking for different time were shown in Figure 2. The average elongation at break and average tensile strength were summarized in Table II. Tensile strength of SF/HBC nanofibrous scaffolds gradually increased from 11.44 ± 1.37 MPa to 39.53 ± 6.29 MPa with increasing crosslinking time from 12 to 72 h. Elongation at break was 3.09% ± 0.37% after the scaffolds were crosslinked for 12 h, later it increased to 8.88% ± 1.42% with a crosslinking period for 24 h. When the time was extended to 72 h, elongation at break gradually deceased from 8.88% ± 1.42% to 5.11% ± 0.84%. This may be because nanofibers were not connected with each other completely after 12 h, scaffolds fractured easily via extruded. Then, the nanofibers were tightly connected each other to some extent leading to suitable mechanical properties after 24 h. With further increasing of crosslinking time, nanofibers were intended to bond together, becoming stiffer but less ductile. The stress–strain curves of crosslinked nanofibrous scaffolds with different crosslinking agents for 24 h were shown in Figure 3, and the average elongation at break and average tensile strength was summarized in Table II. The tensile strength (16.71 ± 0.40 MPa) and elongation at break (3.20% ± 0.37%) of GTA-crosslinked scaffolds were lower than those of genipin-crosslinked scaffolds (18.65 ± 1.22 MPa, 8.88% ± 1.42%) and ethanol-crosslinked scaffolds (21.37 ± 0.55 MPa, 5.45% ± 0.60%). The reason was probably associated with the SF conformation from random coils or α-helix (silk I) to β-sheet (silk II) of crosslinked scaffolds with genipin and ethanol rather than GTA. In a word, the above results elucidated that crosslinked SF/HBC nanofibrous scaffolds with genipin vapor for 24 h possessed better mechanical properties in comparison with other conditions.

Morphology of crosslinked SF/HBC nanofibrous scaffolds

The crosslinking experiments of SF/HBC nanofibous scaffolds at the weight ratio of 20:80 have no good stability. Sometimes, the pore structure was destroyed after crosslinking. So, we selected the SF/HBC nanofibous scaffolds at the weight ratio of 50:50 as following study. SEM micrographs of noncrosslinked electrospun SF/HBC fibers were shown in Figure 4. The continuous bead-free nanofibers were obtained, and the average diameter was 226 nm ± 137 nm. Meanwhile, some ultrafine-threaded fibers could be found among nanofibers. Because chitosan is a typical cationic polyelectrolyte, higher charge density of the solution splited the jet into smaller jets, resulting in ultrathin fibers.[19] The noncrosslinked electrospun SF/HBC fibers are soluble or swollen in water. To potentially use electrospun SF/HBC fibers for tissue engineering, crosslinking is necessary. SEM micrographs of SF/HBC nanofibrous scaffolds after crosslinking with genipin for different time and with GTA and ethanol as well as water resistant tests were shown in Figure 5. Compared to noncrosslinked nanofiers, crosslinked nanofibers were deformed to different degree by the vapor. For the

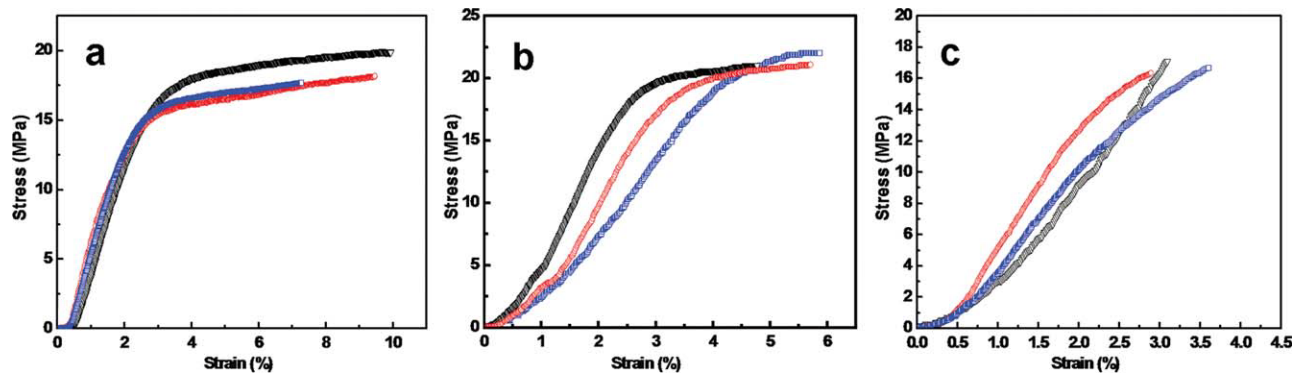

FIGURE 3. The stress-strain curves of SF/HBC nanofibrous scaffolds after crosslinking with different crosslinking agents for 24 h. (a) genipin; (b) ethanol; (c) glutaraldehyde. [Color figure can be viewed in the online issue, which is available at wileyonlinelibrary.com.]

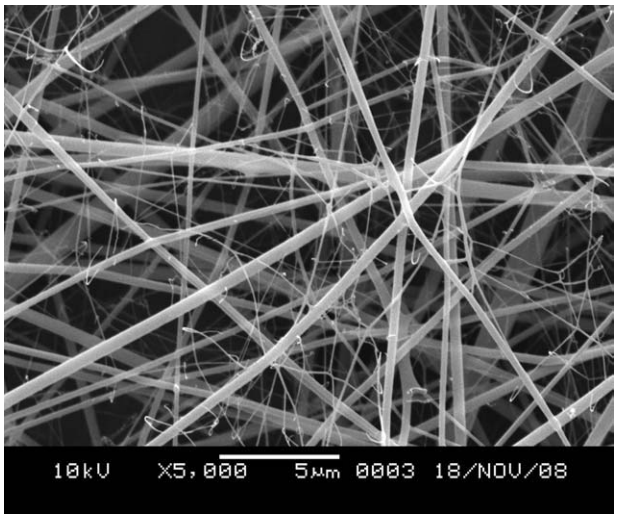

FIGURE 4. SEM photographs of uncrosslinked SF/HBC nanofibrous scaffolds.

water-resistant test in water, micrographs of genipin-crosslinked nanofibers for 12 h completely disappeared, while their counterparts for 24 and 48 h still remained fibrous structure. GTA-crosslinked nanofibers for 24 h remained fibrous structure. Crosslinked nanofibrous scaffolds were required to possess good stability and suitable porosity and pore diameters for cell growth. From long-term consideration, genipin-crosslinked nanofibers scaffolds were beneficial for transplantation *in vivo* as tissue-engineering scaffolds in comparison with GTA crosslinked ones because of the possession of lower cytotoxicity. Compared to genipin and GTA crosslinked nanofibers, micrographs of ethanol-treated nanofibers had smaller changes but nanofibers swelled and original micrographs disappeared after soaking. This may be explained that ethanol just induced transformation from random coil or α-helix to β-sheet of the conformation of SF[20] or inter- and intramolecular H-bonds but not form inter- and intramolecular covalent bonds through crosslinking agents.

Pore diameter distribution and porosity analyses

Electrospun nanofibrous scaffolds with microscale and nanoscale porous structure are most favorable for tissue-engineering scaffolds, because the highly porous network of interconnected pores provides nutrients and gas exchange, which are crucial for cellular growth and tissue regeneration.[21] Pore diameter distribution, pore diameters, and porosities of SF/HBC nanofibrous scaffolds (50:50) after genipin crosslinking with different time along with GTA and ethanol for 24 h were shown in Figure 6 and were summarized in Table III. Before crosslinking, mean flow pore diameter and porosity of nanofibrous scaffolds was 0.2646 ± 0.1355 μm and 90.23%. Compared to crosslinking with genipin for 12 h, higher mean flow pore diameter and porosity appeared, because the noncrosslinked nanofibers loosely packed together. After crosslinked with different time from 12 to 48 h with genipin, mean flow pore diameter of nanofibrous scaffolds increased from 0.1669 ± 0.0463 μm to 0.3073 ± 0.1969 μm and then decreased to 0.1621 ± 0.0970 μm. In this experiment, although nanofibrous scaffolds were fixed by framework, we found nanofibrous scaffolds still shrank slightly and became thinner after crosslinking. Meanwhile, from the above SEM, we can see that the some nanofibers bonded with each other while others deformed by vapor. It was reported that pore size was strongly associated with fiber mass, fiber thickness, fiber diameter, and fiber length. An increase in fiber mass and

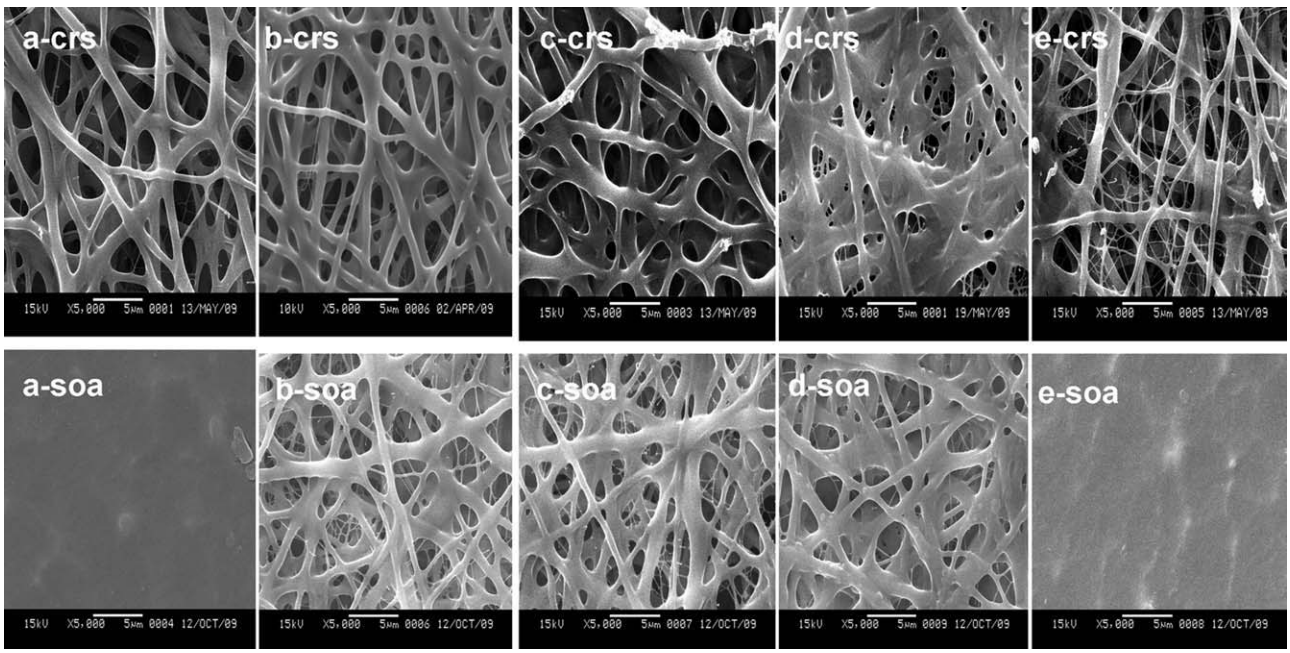

FIGURE 5. SEM photographs of crosslinked (-crs) and soaked (-soa) SF/HBC nanofibrous scaffolds (a) genipin for 12 h; (b) genipin for 24 h; (c) genipin for 48 h; (d) glutaraldehyde for 24 h; (e) ethanol for 24 h.

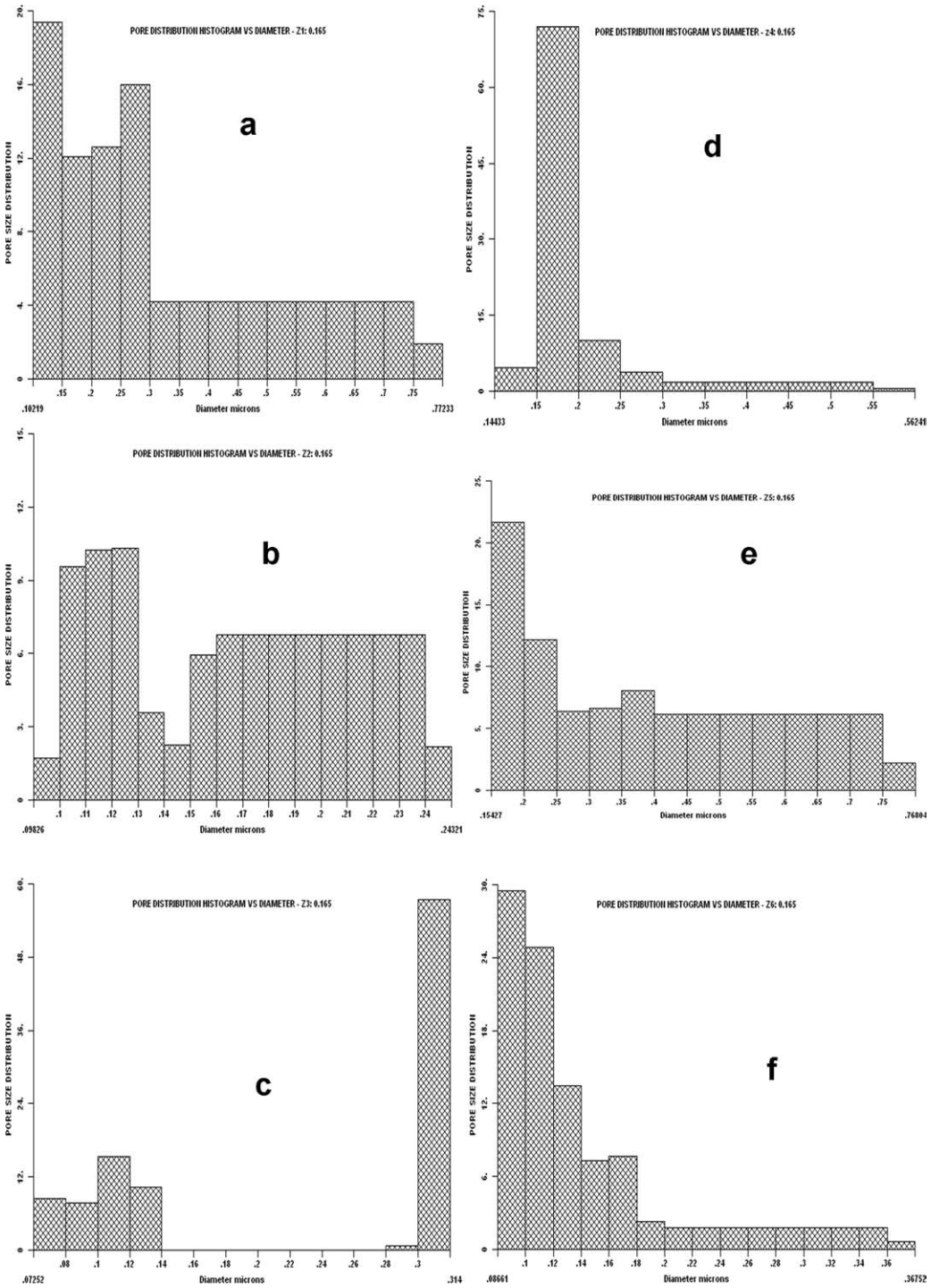

FIGURE 6. Pore diameter distribution of electrospun and crosslinked SF/HBC nanofibrous scaffolds. (a) non-crosslink; (b)12 h (genipin); (c) 24 h (genipin); (d) 48 h (genipin); (e) 24 h (TGA); (f) 24 h (ethanol).

thickness could cause a decrease in pore size. Fiber diameter plays a dominant role in controlling pore diameter of scaffolds, decreasing fiber diameter results in a decrease in mean pore radius.[22] After crosslinking for 12 h, shrinkage of nanofibrous scaffolds might cause the decrease of mean flow pore diameter and porosity. After 24 h of crosslinking, lager nanofibrous diameters were attributed to increase mean flow pore diameter and porosity. Pore diameter distribution shifted larger micron (Fig. 6). After crosslinking for 48 h, the further swelling of nanafibers might result in pore diameter decrease. Meanwhile, GTA-crosskinked nanofibrous scaffold had larger mean flow pore diameter and higher porosity than others. Pore diameter distribution shifted larger micron (Fig. 6). Ethanol-crosslinked nanofibrous scaffold

TABLE III. Pore Diameter and Porosities of SF/HBC Nanofibrous Scaffolds Before and After Crosslinking

Samples	Specimen Thickness (mm)	Mean Flow Pore Diameter ± SD (μm)	Largest Pore Diameter (μm)	Smallest Pore Diameter (μm)	Porosity (%)
Noncrosslinked	0.21	0.2646 ± 0.1355	0.7723	0.1045	90.23
Genipin (12 h)	0.12	0.1669 ± 0.0463	0.2432	0.0983	84.33
Genipin (24 h)	0.15	0.3073 ± 0.1969	0.3140	0.0728	88.92
Genipin (48 h)	0.148	0.1621 ± 0.0970	0.5624	0.1456	86.71
GTA (24 h)	0.145	0.3703 ± 0.1518	0.7680	0.1554	89.50
Ethanol (24 h)	0.198	0.116 ± 0.0552	0.3675	0.0872	86.18

had the lowest mean flow pore diameter and porosity. The crosslinking could cause important changes of nanofibers architecture (including nanofiber diameter, pore diameter distribution, and porosity).

Structure of cross-linked SF/HBC nanofibers

Recently, genipin has been widely used for crosslinking collagen, gelation, chitosan, SF, and their composites and compared with cross linking regents such as GTA, formaldehyde, and epoxy compounds, which assessed genipin lower cytotoxicity and higher biocompatibility.[12,23–25] One mechanism is a nucleophilic attack by an amine group on the olefinic carbon atom at C-3 of deoxyloganin aglycon that eventually leads to the formation of a heterocyclic amine. The intermediate compounds could be further associated to form crosslinked networks with short chains of crosslinking bridges.[26,27] The reaction mechanisms of SF and HBC crosslinked by genipin may be similar to them and are illustrated as follows:

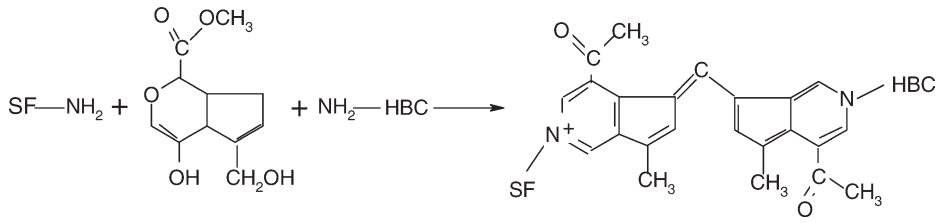

FTIR-ATR spectra of electrospun SF/HBC nanofibers and crosslinked SF/HBC nanofibers with genipin and GTA were shown in Figure 7. Electrospun SF/HBC nanofibers showed absorption bands at 1381, 1135, and 1071 cm^{-1}, which were attributed to the saccharide structure, and at 1671, 1534, 1429, and 1201 cm^{-1}, which were attributed to amide I, amide II, amide III, of SF and the amino group and amide group of HBC.[28–30] After crosslinking with genipin, new absorption band at 1628 cm^{-1} appeared, which was attributed to C=C double bond ring stretch modes of the core of the genipin molecules.[31] Characteristic absorption bands of new bond

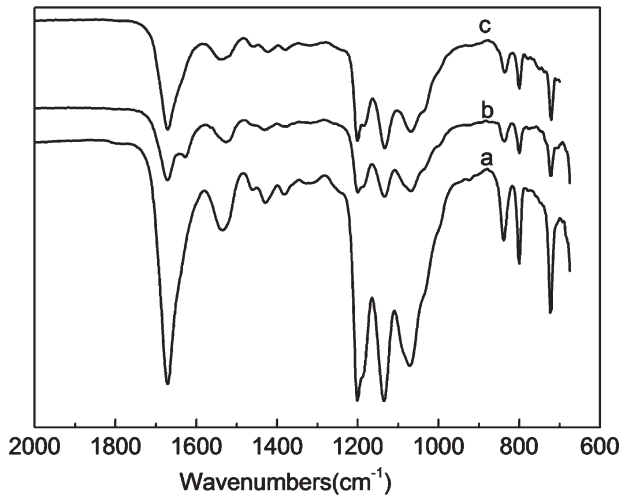

FIGURE 7. FTIR-ATR spectra of electrospun and crosslinked SF/HBC nanofibrous scaffolds. (a) uncrosslinked; (b) genipin-crosslinked; (c) glutaraldehyde-crosslinked.

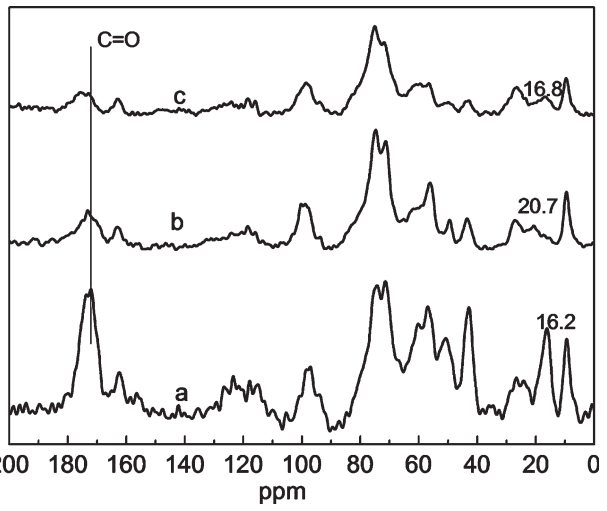

FIGURE 8. 13C CP/MAS NMR spectra of electrospun and crosslinked SF/HBC nanofibrous scaffolds. (a) uncrosslinked; (b) genipin-crosslinked; (c) glutaraldehyde-crosslinked.

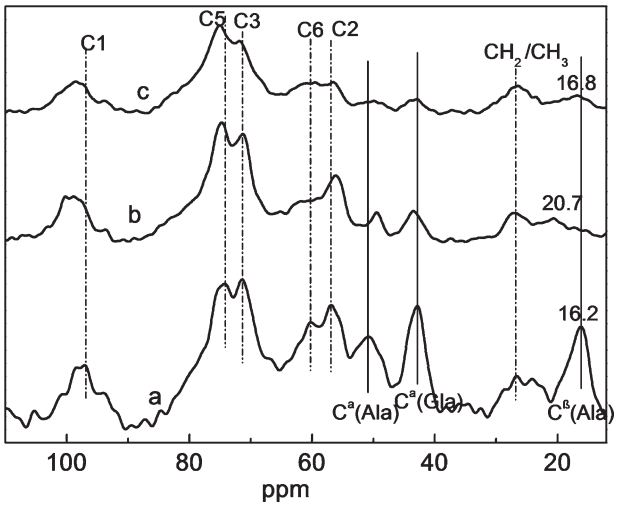

FIGURE 9. Expanded 13C CP/MAS NMR spectra of electrospun and crosslinked SF/HBC nanofibrous scaffolds. (a) uncrosslinked; (b) genipin-crosslinked; (c) glutaraldehyde-crosslinked.

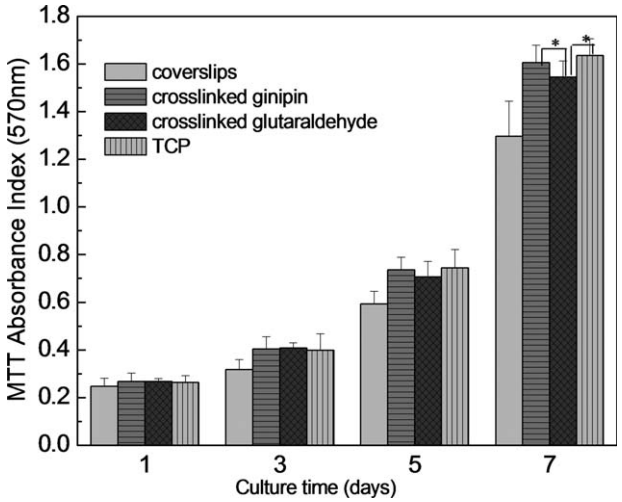

FIGURE 10. Proliferation of PEICs cultured on crosslinked SF/HBC nanofibrous scaffolds with genipin and glutaraldehyde, coverslips, and TCP for 1, 3, 5, and 7 days. Data are expressed as mean ± SD ($n = 4$). Statistical difference between groups is indicated (*$p < 0.05$).

C=N (at 1620–1680 cm^{-1}) and C—N formed by crosslinking reaction overlapped characteristic absorption bands of amide Ior C=C double bond and amide II and amide III, respectively. Thus, these characteristic absorption bands were not observed. Characteristic absorption band of amide II shifted from 1534 cm^{-1} to 1526 cm^{-1}, which was attributed to the change of conformation from random coils or α-helix to β-sheet.[9] After crosslinking with GTA, new characteristic absorption bands were not appeared. Characterization of imine C=N stretching vibration overlapped with the strong absorption of the amide I band in SF and chitosan.

Solid-state ^{13}C NMR has been shown to be a more effective structure analytical tool for polymers including proteins

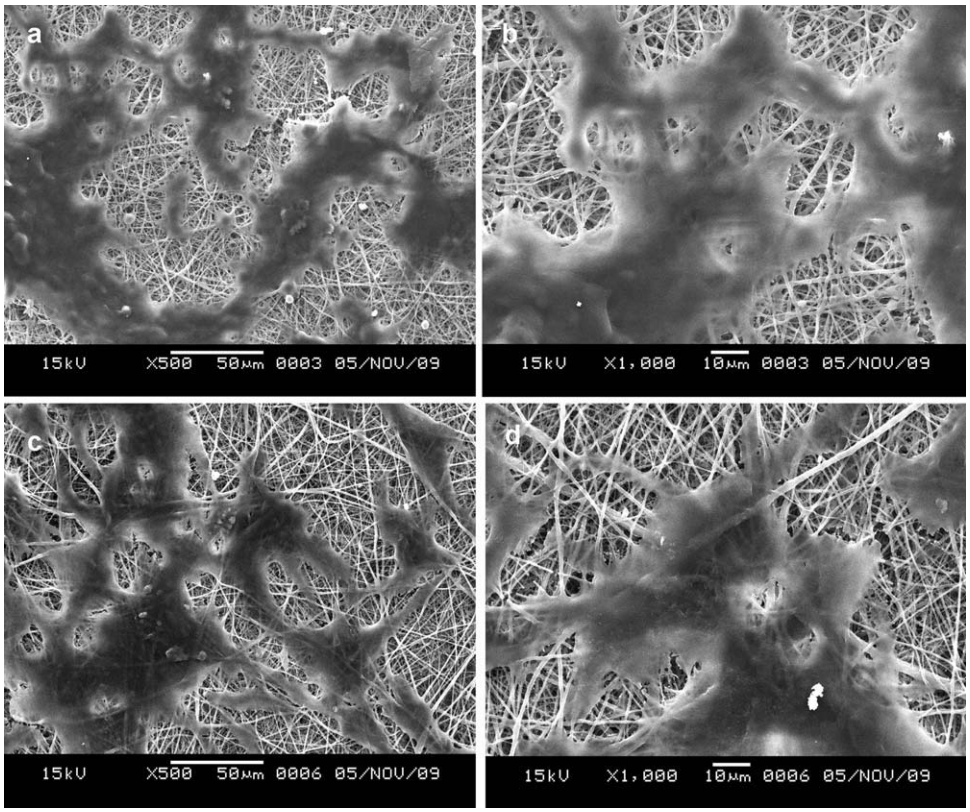

FIGURE 11. SEM micrographs of PEICs grown on crosslinked nanofibrous scaffolds for 3 days. (a, b) Genipin-crosslinked; (c, d) glutaraldehyde-crosslinked.

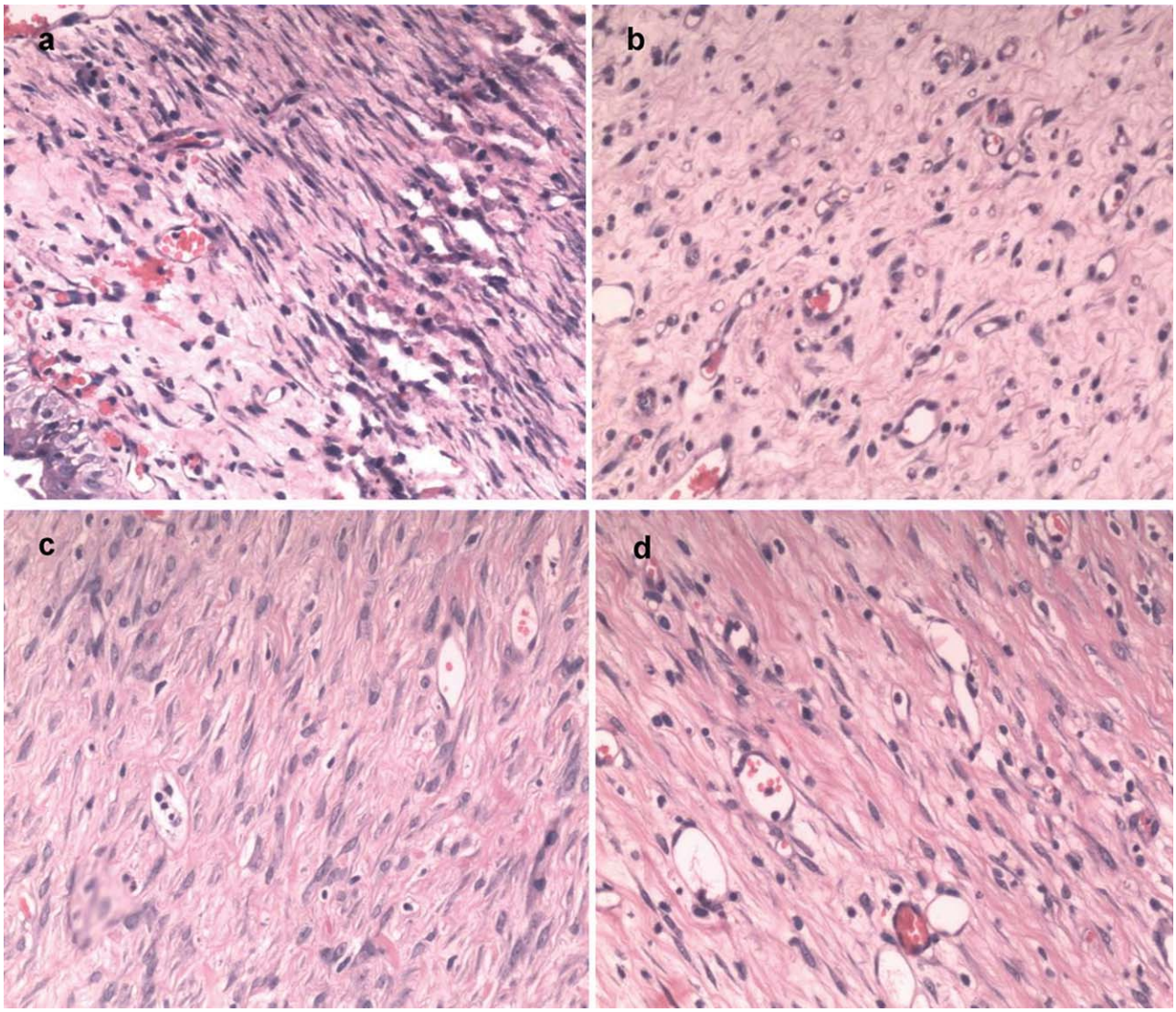

FIGURE 12. Photomicrographs of wound healing of rat skin. (a) SF/HBC nanofibrous scaffolds at 1 week; (b) control group at 1 week; (c) SF/HBC nanofibrous scaffolds at 3 weeks; (d) control group at 3 weeks (H&E, 100). [Color figure can be viewed in the online issue, which is available at wileyonlinelibrary.com.]

due to the sensitivity of isotropic ^{13}C NMR chemical shifts of carbon atomic resolution. To further confirm crosslinking reaction and conformation change, the ^{13}C CP/MAS NMR spectra and expanded ^{13}C CP/MAS NMR spectra of electrospun SF/HBC nanofibers, crosslinked SF/HBC nanofibers with genipin as well as GTA were investigated, and the results were shown in Figures 8 and 9. The chemical shift of Ala C^{β} in SF nanofibers varied from 16.2 ppm for random coils or α-helix to 20.7 ppm for β-sheet conformation after crosslinked by genipin. Zhou et al.[32] illustrated that the chemical shifts in Ala residues of C^{β} within 18.5–20.5 ppm were assigned β-sheet conformation (silk II), the chemical shifts in Ala residues of C^{β} within 14.5–17.5 ppm were assigned to random coils or α-helix (silk I). Meanwhile, chemical shift of carbonyl carbons of SF transform from 172.0 to 173.3 ppm and peak density obviously decreased. Chemical shift of C2 bond NH_2 in HBC, C^{α} bond NH_2 of Gla, and C^{α} bond NH_2 of Ala in SF transformed from 57.1 ppm to 56.4 ppm, from 42.9 ppm to 43.5 ppm, and from 50.8 ppm to 49.4 ppm, respectively, this could be attributed to the reaction of amino groups of SF and HBC with genipin. The results demonstrated that genipin not only induced conformation of SF converted random coil or α-helix to β-sheet but also acted as a crosslinking agent for SF and HBC. After crosslinking with GTA, the peak observed at 175.7 ppm was attributed to the double imine bond (C=N) of the Schiff base,[33] chemical shift of C2 bond NH_2 in HBC, C^{α} bond NH_2 of Gla, and C^{α} bond NH_2 of Ala in SF appeared similar change and peak densities obviously decreased. The results showed that GTA acted as crosslinking agent for SF and HBC. However, the chemical shift of Ala C^{β} in SF nanofibers only varied from 16.2 to 16.8 ppm, indicating that the conformation of SF mainly exist in random coil or α-helix.

Viablity study of cells on nanofibrous scaffolds

The crosslinking treatment could improve the water-resistant ability and mechanical properties of the SF/HBC nanofibrous scaffolds. To evaluate cell attatchment and proliferation on the crosslinked electrospun SF/HBC nanofibrous scaffolds (50:50), PIECs were seeded on the nanofibrous scaffolds. The viability of PIECs on days 1, 3, 5, and 7 after seeding on various nanofibrous scaffolds was shown in Figure 10. It was revealed that all the nanofibrous scaffolds had good cell viability in comparison with coverslips. On days 1, 3, and 5, proliferation on croslinked SF/HBC nanofibrous scaffolds with genipin and GTA exhibited no significant difference. On day 7, proliferation on crosslinked SF/HBC nanofibrous scaffolds with genipin exhibited significant increase ($p < 0.05$) than that of crosslinked GTA. Through thoroughly rinsing the crosslinked material can alleviate maximally the amount of residual GTA molecules at the beginning.[34] Along with culture time increasing, a small quantity of residual GTA may be dissolved in culture medium. Compared to TCP, genipin-crosslinked nanofibrous scaffolds had no significant difference.

Cell morphology and the interaction between cells and electrospun SF scaffolds were studied *in vitro* for 3 days. SEM micrographs were shown in Figure 11. After 3 days, PIECs attached and spread on the surface of crosslinked SF/HBC nanofibrous scaffolds with genipin and GTA and formed confluent endothelial monolayer. From tissue-engineering application for a long time, crosslinked SF/HBC nanofibrous scaffolds with genipin may be superior to those of with GTA.

Histologic examination

In wound-healing tests, full-thickness rectangular wounds were made on the back of each rat. Representative photomicrographs at the wound tissue in the nanofibrous scaffolds (50:50) and the control group were shown in Figure 12. After 1 week, there were inflammatory response in the nanofibers and control groups. Greater proliferation of fibroblasts was observed in the nanofibers than in the control group. After 3 weeks, inflammatory cells obviously decreased in both groups, epithelization of the wound was completed, a proliferation of fibroblasts and thickened collagen fibers were observed, and blood vessels decreased in both groups. Additionally, fibroblast cells had greater proliferation and arranged in better order, densely in comparison with the control. The results clarified that crosslinked SF/HBC nanofibrous scaffolds with genipin possessed good biocompatibility *in vivo*.

CONCLUSIONS

In this study, SF/HBC nanofibrous scaffolds were fabricated via elctrospinning to biomimic natural ECM. To improve stability of SF/HBC nanofibrous scaffolds *in vitro* and *in vivo*, genipin, GTA, and ethanol vapor were used to crosslink electrospun nanofibers, respectively. The results of mechanical test and water resistant test showed that genipin was a more predominant crosslinking agent to crosslink SF/HBC nanofibrous scaffolds in comparison with GTA and ethanol. Moreover, characterization of the microstructure (porosity and pore structure) demonstrated crosslinked nanofibrous scaffolds with genipin and GTA had lager porosities and mean diameters than that with ethanol. Characterization of FTIR-ATR and ^{13}C NMR clarified both genipin and TGA acted as crosslinking agents for SF and HBC. And genipin induced SF conformation from random coil or α-helix to β-sheet. The results of cell-viability studies *in vitro* and wound-healing tests *in vivo* demonstrated that crosslinked SF/HBC nanofibrous scaffolds with genipin possessed good biocompatibity. Although TGA could also successfully crosslink SF/HBC nanofibrous scaffolds, many previous reports revealed that GTA had remained toxicity to a certain extent. From long-term consideration, genipin may be a better method of crosslinking SF/HBC nanofibrous scaffolds for tissue-engineering scaffolds. Ongoing studies will focus on developing tissue-engineering scaffolds for skin and blood vessel.

REFERENCES

1. Xu CY, Inai R, Kotaki M, Ramakrishna S. Aligned biodegradable nanofibrous structure: A potential scaffold for blood vessel engineering. Biomaterials 2004;25:877–886.
2. Min BM, Lee G, Kim SH, Nam YS, Lee TS, Park WH. Electrospinning of silk fibroin nanofibers and its effect on the adhesion and spreading of normal human keratinocytes and fibroblasts in vitro. Biomaterials 2004;25:1289–1297.
3. Wang M, Jin HJ, David L, Rutledge GC. Mechanical properties of electrospun silk fibers. Macromolecules 2004;37:6856–6864.
4. Li WJ, Laurencin CT, Caterson EJ, Tuan RS, Ko FK. Electrospun nanofibrous structure: A novel scaffold for tissue engineering. J Biomed Mater Res 2002;60:613–621.
5. Dang JM, Leong KW. Myogenic induction of aligned mesenchymal stem cell sheets by culture on thermally responsive electrospun nanofibers. Adv Mater 2007;19:2775–2779.
6. Chen BY, Dang JY, Tan TL Fang N, Chen WN, Leong KW, Chan V. Dynamics of smooth muscle cell deadhesion from thermosensitivehydroxybutyl chitosan. Biomaterials 2007;28:1503–1514.
7. Dang JM, Sun DDN, Shin Y, Sieber AN, Kostuik JP, Leong KW. Temperature-responsive hydroxybutyl chitosan for the culture of mesenchymal stem cells and intervertebral disk cells. Biomaterials 2006;27:406–418.
8. Jeong L, Lee KY, Liu JW, Park WH. Time-resolved structural investigation of regenerated silk fibroin nanofibers treated with solvent vapor. Int J Biol Macromol 2006;38:140–144.
9. Min BM, Jeong L, Lee KY, Park WH. Regenerated silk fibroin nanofibers: Water vapor-induced structural changes and their effects on the behavior of normal human cells. Macromol Biosci 2006;6:285–292.
10. Schiffman JD, Schauer CL. Cross-linking chitosan nanofibers. Biomacromolecules 2007;8:594–601.
11. Zhou YS, Yang DZ, Chen XM, Xu Q, Lu FM, Nie J. Electrospun water-soluble carboxyethyl chitosan/poly(vinyl alcohol) nanofibrous membrane as potential wound dressing for skin regeneration. Biomacromolecules 2008;9:349–354.
12. Chiono V, Pulieri E, Vozzi G, Ciardelli G, Ahluwalia A, Giusti P. Genipin-crosslinked chitosan/gelatin blends for biomedical applications. J Mater Sci Mater Med 2008;19:889–898.
13. Hillberg AL, Holmes CA, Tabrizian M. Effect of genipin crosslinking on the cellular adhesion properties of layer-by-layer assembled polyelectrolyte films. Biomaterials 2009;30:4463–4470.
14. Tsai CC, Huang RN, Sung HW, Liang HC. In vitro evaluation of the genotoxicity of a naturally occurring crosslinking agent (genipin) for biologic tissue fixation. J Biomed Mater Res 2000;52:58–65.
15. Silva SS, Motta A, Rodrigues MT, Pinheiro AFM, Gomes ME, Mano GF, Reis RL, Migliaresi C. Novel genipin-cross-linked

chitosan/silk fibroin sponges for cartilage engineering strategies. Biomacromolecules 2008;9:2764–2774.
16. Yang MC, Wang SS, Chou NK, Chi NH, Huang YY, Chang YL, Shieh MJ, Chung TW. The cardiomyogenic differentiation of rat mesenchymal stem cells on silk fibroin-polysaccharide cardiac patches in vitro. Biomaterials 2009;30:3757–3765.
17. He W, Yong T, Teo WE, Ma ZW, Ramakrishna S. Fabrication and endothelialization of collagen-blended biodegradable polymer nanofibers: Potential vascular graft for blood vessel tissue engineering. Tissue Eng 2005;11:1574–1588.
18. Huang ZM, Zhang YZ, Ramakrishna S, Lim CT. Electrospinning and mechanical characterization of gelatin nanofibers. Polymer 2004;45:5361–5368.
19. Subbiah T, Bhat GS, Tock RW, Parameswaran S, Ramkumar SS. Electrospinning of nanofibers. J Appl Polym Sci 2005;96:557–569.
20. Chen X, Shao ZZ, Marinkovic NS, Miller LM, Zhou P, Chance MR. Conformation transition kinetics of regenerated Bombyx mori silk fibroin membrane monitored by time-resolved FTIR spectroscopy. Biophys Chem 2001;89:25–34.
21. Eichhorn SJ. Sampson WW. Statistical geometry of pores and statistics of porous nanofibrous assemblies. J R Soc Interf 2005;2: 309–318.
22. Li DP, Frey MW, Joo YL. Characterization of nanofibrous membranes with capillary flow porometry. J Membr Sci 2006;286: 104–114.
23. Silva SS, Maniglio D, Motta A, Mano JF, Reis RL, Migliaresi C. Genipin-modified silk-fibroin nanometric nets. Macromol Biosci 2008;8:766–774.
24. Sundararaghavan HG, Monteiro GA, Lapin NA, Chabal YJ, Miksan JR, Shreiber DI. Genipin-induced changes in collagen gels: Correlation of mechanical properties to fluorescence. J Biomed Mater Res A 2008;87:308–320.
25. Sung HW, Chang Y, Chiu CT, Chen CN, Liang HC. Crosslinking characteristics and mechanical properties of a bovine pericardium fixed with a naturally occurring crosslinking agent. J Biomed Mater Res A 1999;47:116–126.
26. Sung HW, Chen CN, Huang RN, Hsu JC, Chang WH. In vitro surface characterization of a biological patched with a naturally occurring crosslinking agent. Biomaterials 2000;21:1353–1362.
27. Mi FL, Sung UW, Shyu SS. Synthesis and characterization of a novel chitosan-based network prepared using naturally occurring crosslinker. J Polym Sci Part A: Polym Chem 2000;38: 2804–2814.
28. Kweon A, Ha HC, Um IC, Park YH. Physical properties of silk fibroin/chitosan blend films. J Appl Polym Sci 2001;80:928–934.
29. Magoshi J, Mizuide M, Magoshi Y. Physical properties and structure of silk conformational changes in silk fibroin induced by immersion in water at 2 to 130°C. J Polym Sci: Polym Phys Ed 1979;17:515–520.
30. Chen X, Shao ZZ, Marinkovic NS, Miller LM, Zhou P, Chance MR. Conformation transition kinetics of regenerated Bombyx mori silk fibroin membrane monitored by time-resolved FTIR spectroscopy. Biophys Chem 2001;89:25–34.
31. Touyama R, Takeda Y, Inoue K, Kawamura I, Yatsuzuka M, Ikumoto T, Shingu T, Yokoi T, Inouye H. Studies on the blue pigments produced from genipin and methylamine. I. Structures of the brownish-red pigments, intermediates leading to the blue pigments. Chem Pharm Bull 1994;42:668–673.
32. Zhou P, Li GY, Shao ZZ, Pan XY, Yu TY. Structure of Bombyx mori silk fibroin based on the DFT chemical shift calculation. J Phys Chem B 2001;105:12469–12476.
33. Oyrton AC, Monteiro J, Claudio A. Some studies of crosslinking chitosan-glutaraldehyde interaction in a homogeneous system. Int J Biol Macromol 1999;26:119–128.
34. Zhang YZ, Venugopal J, Huang ZM, Lim CT, Ramakrishna S. Crosslinking of the electrospun gelatin nanofibers. Polymer 2006;47:2911–2917.